Temporal dynamics of GABA and Glx in the visual cortex

Reuben Rideaux
Department of Psychology, Downing Street, University of Cambridge, CB2 3EB, UK
reuben.rideaux@gmail.com

ABSTRACT

Magnetic resonance spectroscopy (MRS) can be used in vivo to quantify metabolite concentration and provide evidence for the involvement of different neurotransmitter systems, e.g., inhibitory and excitatory, in sensory and cognitive processes. The relatively low signal-to-noise of MRS measurements has shaped the types of questions that it has been used to address. In particular, temporal resolution is often sacrificed in MRS studies to achieve sufficient signal to produce a reliable estimate of metabolite concentration. Here we apply novel analyses with large datasets to reveal the dynamics of GABA+ and Glx in the visual cortex while participants are at rest (with eyes closed) and compare this with changes in the posterior cingulate cortex. We find that the dynamic concentration of GABA+ and Glx in the visual cortex drifts in opposite directions, that is, GABA+ decreased while Glx increases over time. Further, we find that in the visual cortex, the concentration of GABA+ predicts that of Glx, such that a change in GABA+ is correlated with a subsequent opposite change in Glx. Together, these results expose novel temporal trends and interdependencies of primary neurotransmitters in the visual cortex. More broadly, we demonstrate the feasibility of using MRS to investigate in vivo dynamic changes of metabolites.

Keywords: Magnetic resonance spectroscopy; visual cortex; GABA; Glx; temporal dynamics

INTRODUCTION

Magnetic resonance spectroscopy (MRS) can be used in vivo to measure the concentration of metabolites within the brain. Whereas the blood-oxygen-level-dependent signal measured using functional magnetic resonance imaging (fMRI) cannot distinguish between different systems of activity, e.g., excitatory and inhibitory, measuring the concentration of neurotransmitters within the brain with MRS can begin to differentiate between these systems. For the purpose of understanding neural mechanisms, identifying the involvement of neurotransmitter systems that support sensory/cognitive processes can be more informative than locating regions of neural representation.

The methodological approaches used to investigate sensory/cognitive processing with MRS can be separated into two categories: correlational and functional. The common correlational approach is to measure the concentration of metabolites in a group of participants, within a brain region of interest, and test whether individual variance of a particular metabolite is related to performance on a task supported by the sensory/cognitive process. For example, concentration of the inhibitory neurotransmitter γ-aminobutyric acid (GABA) in the visual cortex is inversely related with visual discrimination of orientation (Edden et al., 2009; Kurcyus et al., 2018; Mikkelsen et al., 2018a). This finding has been interpreted as indicating that sharp neuronal tuning for orientation is supported by inhibition.

A common functional approach used to identify metabolite involvement is to measure baseline metabolite concentration while a participant is “at rest” and compare this with another measurement taken while the participant performs a task. A difference metabolite concentration observed between the two measurements may be taken as evidence of its involvement in the sensory/cognitive processes supporting the task. For example, GABA concentration in the visual cortex is different when participants view stereoscopic images composed of both light and dark features, compared to just light or dark features (Rideaux et al., 2019). This has been interpreted as evidence for the increased involvement of inhibition in visual processing of combined light and dark features.

Another functional approach is also used, in which the second measurement is taken following (rather than during) the event or activity. For example, Lunghi et al. (2015b) measured GABA concentration in the human visual cortex before and after a period of monocular deprivation and found a reduction. This finding is consistent with previous work in humans (Boroojerdi et al., 2001, 2000; Lunghi et al., 2015a) and mice (He et al., 2006; Huang et al., 2010) showing increased excitability in the visual cortex following a period of (monocular/binocular) visual deprivation, and suggest that there are dynamic changes in GABA in the visual cortex during periods of visual deprivation.

While MRS can be used to differentiate excitatory and inhibitory transmission within the brain, compared to fMRI it is severely limited in terms of its temporal resolution, which is constrained by the signal-to-noise ratio of measurements acquired using the technique. Although the duration that restricts the temporal resolution of MRS (i.e., the relaxation time) can be similar to that of fMRI (i.e., ~2s), in order to yield a reliable measurement of metabolite concentration from within the brain, multiple transients must be combined to reach a sufficient signal-to-noise ratio (Mikkelsen et al., 2018b). For example, it is common to combine between 200-300 transients (~10 min) to produce a single measure of metabolite concentration (Puts and Edden, 2012). This approach, while often necessary, obscures dynamic changes in metabolite concentration that occur during this period.

Here we overcome the signal-to-noise limitation of MRS by applying temporal analyses of metabolite concentration to a large dataset of participants. We measure the dynamic concentration of GABA and Glx in the visual cortex of human participants while at rest (with closed eyes), from a dataset containing 69 scans. We compare these results with data from the posterior cingulate cortex of 196 participants at rest (Mikkelsen et al., 2019, 2017). To observe the dynamics of metabolites, we process the data in two ways. We first take a moving average of a ~6 min period, which reveals low frequency trends in the data consistent with previous work (Lunghi et al., 2015b); that is, GABA reduces and Glx increases. Next, using a new technique, we combine data across participants (rather than time), which allows us to track the concentration of metabolites with relatively high temporal resolution (12 sec) over a 13 min period. This novel approach exposes large changes in GABA+ and Glx, previously obscured by averaging over long durations. Further, we reveal a striking relationship between GABA+ and Glx in the visual cortex: a change in GABA+ predicts the opposite change in Glx both ~30 and ~120 sec later.

The relative low signal-to-noise of MRS has shaped the approaches with which the technique has been used to study the brain. Here we overcome this limitation by using a new technique that combines measurements across a large sample of data, which reveals novel dynamic trends and interactions within and between neurotransmitters.

METHODS

Participants

Fifty-eight healthy participants from the University of Cambridge with normal or corrected-to-normal vision participated in the experiment. The mean age was 24.4 yr (range = 19.4–40.5 yr; 31 women). Nine of the participants, including the author (RR), repeated the experiment twice and one participant repeated three times, on different days; thus, the total number of scans was sixty-nine. Participants were screened for contra-indications to MRI prior to the experiment. All experiments were conducted in accordance with the ethical guidelines of the Declaration of Helsinki and were approved by the University of Cambridge ethics committee and all participants provided informed consent.

Data collection

Participants underwent a MR spectroscopic acquisition targeting the visual cortex at the Cognition and Brain Sciences Unit (Cambridge, UK). During the acquisition, the lights in the room were turned off and participants were instructed to close their eyes. To compare these with data measured from another brain region, we reanalysed previously gathered MR spectroscopic data targeting the posterior cingulate cortex (Mikkelsen et al., 2019, 2017). For the purpose of further comparison, we also reanalysed data from a study investigating metabolite concentrations in the visual cortex under different viewing conditions (Kurcyus et al., 2018).

Data acquisition

Magnetic resonance scanning targeting visual cortex was conducted on a 3T Siemens Prisma equipped with a 32-channel head coil. Anatomical T1-weighted images were acquired for spectroscopic voxel placement with an ‘MP-RAGE’ sequence. For detection of GABA+ (GABA and co-edited macromolecules) and Glx (a complex comprising Glutamate and Glutamine), spectra were acquired using a MEGA-PRESS sequence (Mescher et al., 1998, 1996): TE=68 ms, TR=3000 ms; 256 transients of 2048 data points were acquired in 13 min experiment time; a 14.28 ms Gaussian editing pulse was applied at 1.9 (ON) and 7.5 (OFF) ppm; water unsuppressed 16 transients. Water suppression was achieved using variable power with optimized relaxation delays (VAPOR; Tkáč and Gruetter, 2005) and outer volume suppression (OVS). Automated shimming followed by manual shimming was conducted to achieve approximately 12 Hz water linewidth.

The “Big GABA” dataset comprises a collection of MRS datasets collected by different groups using the same parameters on GE, Phillips, and Siemens scanners. The following data from the Big GABA dataset was used in the current study: G4, G5, G7, G8, P1, P3, P4, P5, P6, P7, P8, P9, P10, S1, S6, & S8; the letter in the notion refers to the scanner make and the

number refers to the group that collected the data. With the exception of G1 and G6, this includes all the available Big GABA datasets. We used the macromolecule unsuppressed transients from these datasets for closer comparison with the visual cortex data, and we excluded data from G1 and G6 as these had fewer transients. A detailed description of the data acquisitions for these datasets can be found in Mikkelsen et al. (2019, 2017). To summarize the procedure, magnetic resonance scanning targeting posterior cingulate cortex was conducted on 3T Siemens, GE, and Phillips scanners equipped with 8-, 32-, or 64-channel head coils. Spectra were acquired using a MEGA-PRESS sequence: TE=68 ms, TR=2000 ms; 320 transients of either 2048 or 4096 data points were acquired in 12 min experiment time; a 15 ms Gaussian editing pulse was applied at 1.9 (ON) and 7.5 (OFF) ppm.

Spectra were acquired from a location targeting visual cortex, i.e., V1/V2 (**Fig. 1a**), and posterior cingulate cortex (**Fig. 1b**). The voxel targeting the visual cortex (3×3×2 cm) was placed medially in the occipital lobe; the lower face aligned with the cerebellar tentorium and positioned so to avoid including the sagittal sinus and to ensure it remained within the occipital lobe. The voxel targeting the posterior cingulate cortex (3×3×3 cm) was positioned in the medial parietal lobe and rotated in the sagittal plane to align with a line connecting the genu and splenium of the corpus callosum. The coordinates of the voxel location were used to draw a mask on the anatomical T1-weighted image to calculate the volume of grey matter (GM), white matter (WM), and cerebral spinal fluid (CSF) within each voxel. Segmentation was performed using the Statistical Parametric Mapping toolbox for MATLAB (SPM12, http://www.fil.ion.ucl.ac.uk/spm/).

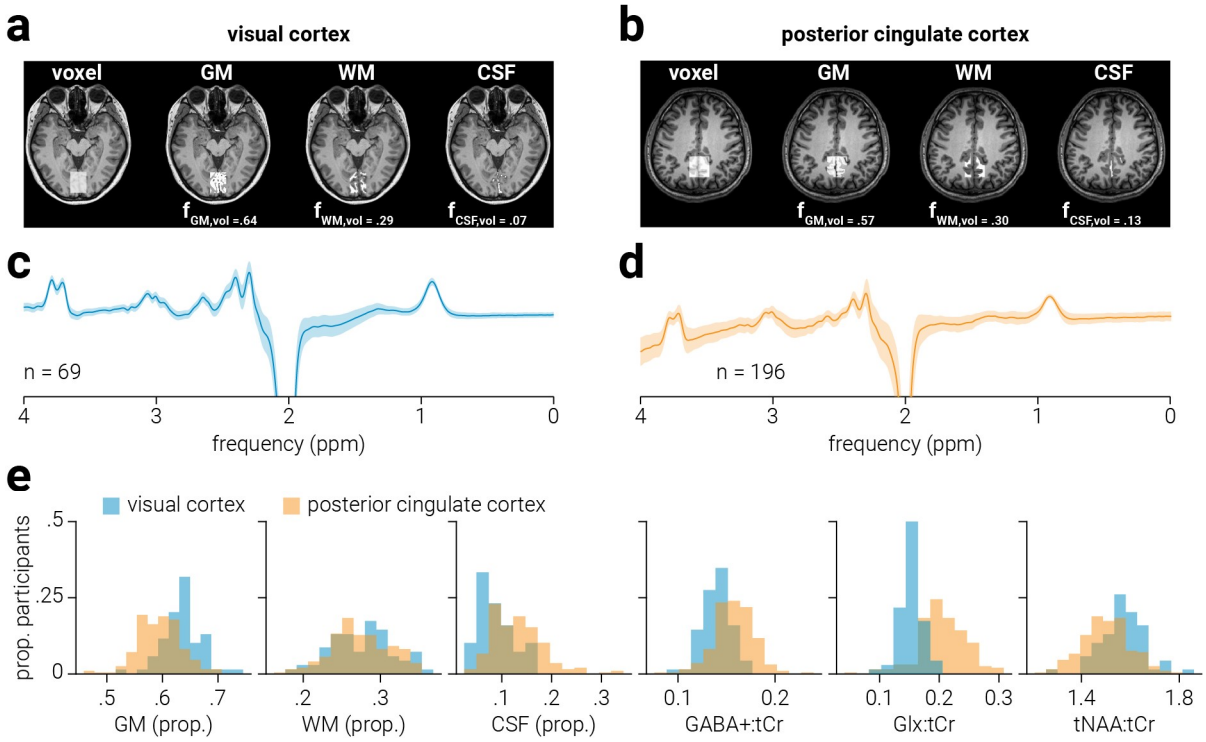

Figure 1. Data acquisition. Representative MRS voxel placement for **a**) visual and **b**) posterior cingulate cortices on a T1-weighted structural image and probabilistic partial volume voxel maps following tissue segmentation for one participant. Corresponding tissue proportions of grey matter (GM), white matter (WM) and cerebrospinal fluid (CSF) are shown. Average spectra across all subjects for **c**) visual and **d**) posterior cingulate cortices; number of subjects comprising each average spectrum is shown and grey shaded regions indicate standard deviation. **e**) Distribution of (GM, WM, CSF) voxel tissue proportions, and (GABA+, Glx, tNAA) metabolite concentrations across participants for visual and posterior cingulate cortices.

In addition to the abovementioned primary datasets, we also reanalysed a subset of the data from Kurcyus et al. (2018); scans for which the authors had access to in individual transient format (as opposed to average of all transients across the scan). The dataset we reanalysed comprised 29, 27, and 28 measurements from an MRS voxel targeting V1, while participants had their eyes closed, open in darkness, or open while viewing an alternating checkerboard stimulus, respectively. A detailed description of the data acquisitions is provided in Kurcyus et al. (2018). To summarize the procedure, magnetic resonance scanning targeting visual cortex was conducted on a 3T Siemens Biograph mMR system equipped a 12-channel head coil. Spectra were acquired using a MEGA-PRESS sequence: TE=68 ms, TR=2000 ms; 256 transients of 2048 data points were acquired in 8.6 min experiment time; editing J-refocusing pulse irradiated at 1.9 (ON) and 7.5 (OFF) ppm.

Data processing

Spectral quantification was conducted in MATLAB using GANNET v3.1 (www.gannetmrs.com; Edden et al., 2014) and in-house scripts. Frequency, phase, area, and full width at half maximum (FWHM) parameters of the Creatine peak at 3.0 ppm were

estimated by fitting a Lorentzian peak to the data and individual spectra with parameter estimates >3 std from the mean were omitted from further analysis; the remaining spectra were frequency and phase corrected using these parameters. Total creatine (tCr) and total N-acetylaspartate (tNAA) signal intensity were determined by fitting a single Lorentzian peak to the mean OFF spectra at 3 ppm and 2 ppm, respectively. ON and OFF spectra were subtracted to produce the edited spectrum (**Fig. 1c** & **d**), from which GABA+ (3 ppm) and Glx (3.8 ppm) signal intensity were modelled off single- and double- Gaussian peaks, respectively. All metabolite signal intensities were calculated as the area of the fitted peak/s.

Intensities of GABA+, Glx, and tNAA were normalized to the commonly used internal reference tCr (Jansen et al., 2006), yielding relative concentration values (i.e., GABA+:tCr, Glx:tCr, and tNAA:tCr; **Fig. 1e**). The tCr signal is acquired within the same MEGA-PRESS transients as the target metabolites. Thus, normalization of GABA+, Glx, and tNAA to tCr minimizes the influence of changes that occur during the acquisition which alter the entire spectrum (e.g., changes in signal strength, line width, chemical shift displacement, or dilution associated with changes in blood flow (Ip et al., 2017)) this will produce no change in the ratio of target metabolites to tCr. For the correlational analyses reported in **Table 2**, a GM correction(Harris et al., 2015) was applied to the metabolite measurements with the following equation:

$$C_{tisscorr} = \frac{C_{meas}}{f_{GM}} \quad (1)$$

where $C_{tisscorr}$ and C_{meas} are the GM-corrected and uncorrected metabolite concentrations (e.g., GABA+:tCr), respectively, and f_{GM} is the proportion of GM within the voxel. All other analyses report concentrations as a proportion of their initial magnitude, and thus do not require tissue correction.

Low resolution dynamic analysis

For the low-resolution dynamic analysis of the visual cortex data, we used a sliding window (width, 128 transients; step size, 2 transients) to measure average metabolite concentration as it changed over the course of the scan (256 transients/768 sec). For the posterior cingulate cortex data, we matched the duration of the sliding window width to the that used for the visual cortex data by including more transients (width, 192 transients; step size, 2 transients), and measured metabolite concentrations as they changed over the course of the scan (320 transients/640 sec). Prior to running analyses, metabolite concentration data were screened to remove noisy and/or spurious quantifications. In particular, we omitted the traces of subjects for which the concentration changed by more than 50% (GABA+/Glx) or 5% (tCr/tNAA) or the standard deviation was greater than three standard deviations from the average standard deviation. This resulted in omission of data from three and five subject's

data in the primary visual and posterior cingulate cortices analyses, respectively. This also resulted in omission of data from zero, two, and one subject's data from the secondary (closed, open, and stimulus) visual cortex analyses (Kurcyus et al., 2018). To remove spurious significant differences in the time course, a cluster correction was applied. Clusters were defined by the sum of their constituent *t*-values and compared to a null hypothesis distribution of clusters produced by shuffling the time labels (5000 permutations); positive and negative *t*-value clusters were treated separately. Clusters below the 95th percentile of the null hypothesis distribution were disregarded.

High resolution dynamic analysis

The temporal resolution of MRS is severely limited by the signal-to-noise ratio of individual spectra. That is, to achieve the signal-to-noise ratio required to yield an accurate metabolic measurement, many individual spectra must be combined. In order to achieve sufficiently high signal in the low-resolution dynamic analysis, we combined multiple (128) spectra within the same subject. This method produces a dynamic trace for each participant; however, the smoothing produced by the sliding window approach may obscure both the true magnitude of metabolic change over time and dynamic changes occurring at higher frequency. Thus, to achieve higher temporal resolution, we averaged individual ON and OFF spectra across participants to produce a single trace (temporal resolution, 4 transients), with no smoothing, for each condition. Note, due to the necessity of large a sample size, this analysis was only performed with the primary datasets. Prior to running analyses, metabolite concentration data were screened to remove noisy and/or spurious quantifications. Specifically, we removed relative concentration values (GABA+/Glx:tCR) that were more than three standard deviations from the mean. This resulted in omission of two GABA+:tCr data points from the posterior cingulate cortex analysis.

To test for predictive relationships between GABA+ and Glx, we ran a cross-correlation analysis between the abovementioned high resolution metabolite traces. We tested for relationships in both directions, that is, whether GABA+ concentration predicts Glx concentration and vice versa. The metabolite traces comprise a limited number of time points (visual cortex: 64, posterior cingulate cortex: 80) and there is an inverse relationship between the lag separating the metabolites and the number of time points included in the cross correlation analysis. This results in less reliable correlation values at lags close to the maximum duration of the metabolite traces due to insufficient sample sizes. To avoid these unreliable correlations, we only included lags with a minimum of 25 time points in the analysis (Bonett and Wright, 2000). This yielded a total of 40 correlations for each predictive direction between GABA+ and Glx in the visual cortex and 56 for the posterior cingulate cortex. To remove spurious significant correlation values in the cross-correlation analyses, a cluster

correction was applied. Clusters were defined by the sum of their constituent *t*-values and compared to a null hypothesis distribution of clusters produced by shuffling the time labels (5000 permutations); positive and negative *t*-value clusters were treated separately. Clusters below the 95th percentile of the null hypothesis distribution were disregarded.

RESULTS

Spectra quality

Table 1 shows the average FWHM (Hz), frequency drift and fitting error for measurements taken from the visual cortex (VC) and posterior cingulate cortex (PCC) from the primary datasets. For each subject, the FWHM was calculated from the average spectra, i.e., spectra averaged across all transients. Frequency drift was calculated as the standard deviation of the position of the Cr peak across individual OFF spectra, prior to alignment; the frequency drift values shown in **Table 1** reflect the average standard deviation across participants. The fitting error for GABA+, Glx, tNAA, and tCr were divided by the amplitude of their fitted peaks to produce normalized measures of uncertainty. The average fit error for each metabolite was relatively low (Mullins et al., 2014) (**Table 1**). One outlier was omitted from the posterior cingulate cortex dataset prior to calculation of the summary statistics shown in **Table 1**.

Table 1. Measures of spectral quality and fit error

Location	FWHM (Hz)				Frequency drift	Fit error			
	GABA+	Glx	tNAA	tCr	(ppm std)	GABA+	Glx	tNAA	tCr
VC	21.6±1.2	17.8±0.4	8.7±1.4	8.7±1.5	0.0088±0.004	10.1±2.2	1.3±0.3	3.6±0.2	3.6±0.2
PCC	20.1±1.5	16.7±0.6	8.2±0.8	7.6±0.6	0.0063±0.006	8.1±0.2	1.8±0.1	3.1±0.1	4.6±0.1

Note: values indicate across subject averages ± standard deviation.

Low resolution temporal dynamics of GABA and Glx

Using a sliding temporal window analysis, we quantified change in the concentration of GABA+ and Glx measured from MRS voxels targeting visual and posterior cingulate cortices over the course of 13 and 12 min periods, respectively. We found that in the visual cortex GABA+ significantly decreased (max difference=-4.5%, $t_{(66)}$=-3.71, P=4.3e^{-4}) while Glx significantly increased (max difference=2.1%, $t_{(66)}$=3.4, P=.001) over the course of the period (**Fig. 2a**). By comparison, we found that in the posterior cingulate cortex there was no significant change in either GABA or Glx (**Fig. 2b**). Given that we referenced GABA+ and Glx to tCr, a possible concern is that the changes in metabolite concentration observed in the visual cortex reflect changes in tCr, as opposed to GABA+ or Glx. However, this is unlikely as we did not find similar changes in tNAA, which was also referenced for tCr (**Fig. 2a**).

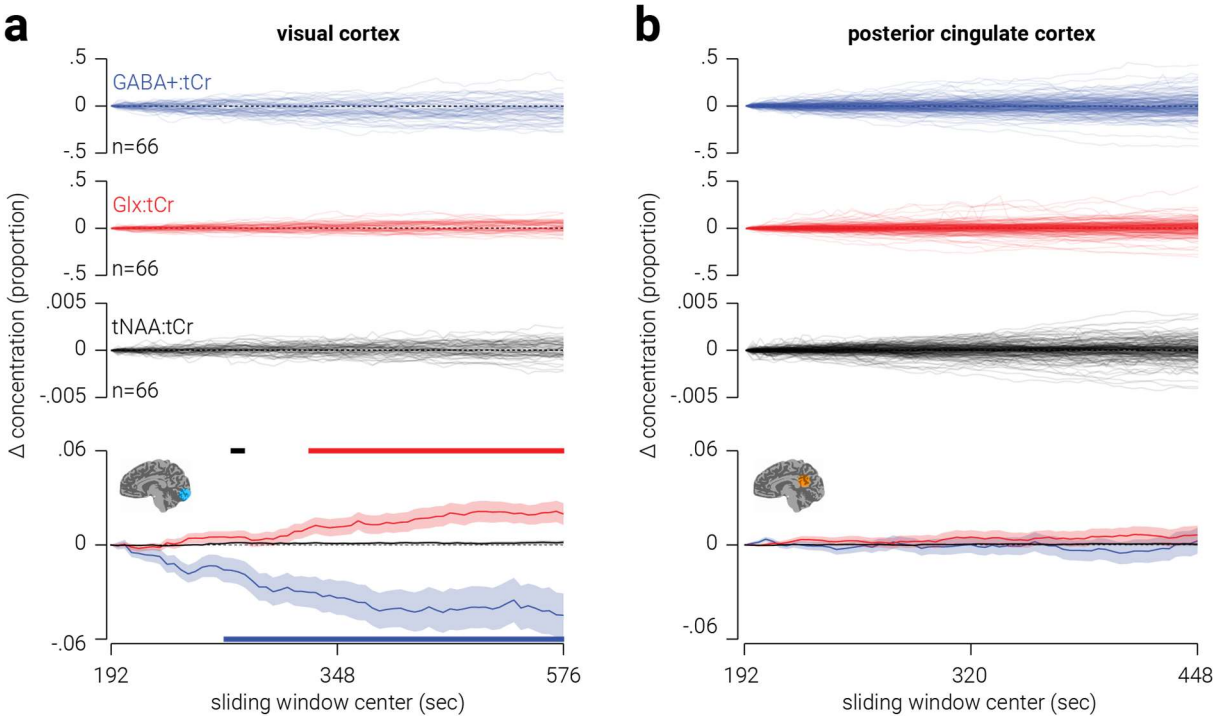

Figure 2. Low resolution temporal dynamics of metabolites in visual and posterior cingulate cortex. (**a**, top) Individual traces showing change in GABA+, Glx, and tNAA (all referenced to tCr) measured from a MRS voxel targeting the visual cortex. (**a**, bottom) Same as (**a**, top), but averaged across participants. (**b**) Same as (**a**), but from a MRS voxel targeting the posterior cingulate cortex. Shaded regions indicate s.e.m. and horizontal coloured bars at the top and bottom of (**a**) indicate (cluster corrected) periods of significant difference from zero.

Another possible concern is that changes observed in the difference spectra over time are related to scanner field drift due to gradient cooling(Lange et al., 2011) or participant motion(Bhattacharyya et al., 2007). In particular, if the scanner field drifts, the position of the editing pulse (1.9 ppm) relative to the GABA (3.0 ppm) and Glx (3.8 ppm) peaks changes. This may change the efficiency with which the peaks are edited and thus their magnitude in the difference spectrum. As the frequency drift of the spectra was relatively low (<0.01 ppm std; **Table 1**), this seems an unlikely explanation. Further, if the scanner field drifted, the position of the editing pulse relative to the GABA and Glx peaks would shift in the same direction for both metabolites. This would produce either a reduction or increase in the magnitude of both peaks. Thus, as we found GABA and Glx concentration changes in opposite directions over time, this cannot be explained by a drift in the scanner field. However, it is possible that changes in one of the metabolites could be accounted for by scanner field drift. As a further test of this possibility, we measured the tNAA trough in the difference spectra using an inverse Lorentzian. Like the magnitude of the GABA+ and Glx peaks, the magnitude of the tNAA trough reflects the efficiency of the editing pulse. Thus, if scanner drift is responsible for changes in the magnitude of the GABA+ or Glx peaks, we would expect to see

corresponding changes in the amplitude of the edited tNAA trough. However, we found no evidence for change in the amplitude of the edited tNAA trough over time.

For each voxel location, we assessed whether there were relationships between different static metabolite concentrations or changes in different concentrations. For static measurements, we averaged across all 256/320 transients. The results of the analysis are shown in **Table 2**. For static metabolite concentrations, we found a positive relationship between Glx and tNAA measured from both visual and posterior cingulate cortices. We also found a positive correlation between GABA+ and tNAA in the visual cortex, and between GABA+ and Glx in the posterior cingulate cortex. By contrast, we found no relationships between the change in different metabolite concentrations.

Table 2. Correlation coefficients between metabolites measured from visual and posterior cingulate cortices

Location	GABA+ & Glx	GABA+ & tNAA	Glx & tNAA	ΔGABA+ & ΔGlx	ΔGABA+ & ΔtNAA	ΔGlx & ΔtNAA
VC	-0.10	0.32**	0.38**	0.03	-0.19	0.10
PCC	0.25***	0.49***	0.17	0.05	-0.05	-0.08

Note: Correlation coefficients are partial coefficients after controlling for the common reference metabolite tCr; VC and PCC denote visual and posterior cingulate cortex; all metabolites are referenced to tCr and tissue-corrected; single, double, and triple asterisks indicate P<.05, P<.01, and P<.001, respectively.

Previous MRS work compared static measurements of GABA+ and Glx concentration taken from a voxel targeting the visual cortex while participants either had their eyes closed, open in the darkness, or open while viewing a dynamic checkerboard stimulus(Kurcyus et al., 2018). This work revealed that GABA+ concentrations were higher when participants had their eyes closed, compared to open in darkness, while Glx concentration was lower when participants' eyes were closed, compared to when receiving visual stimulation. We did not acquire data from participants under different viewing conditions; however, we found that the concentration of GABA+ and Glx changed over the course of the scan when participants had their eyes closed. As a further test of this result, we reanalysed the data from Kurcyus et al. (2018)(Kurcyus et al., 2018), henceforth referred to as the K-dataset, using our dynamic sliding analysis.

As a sanity check, we first analysed the K-dataset using the standard static analysis, replicating the pattern of results found in the previous study (**Fig. 3a-b**; Kurcyus et al., 2018). Additionally, we applied this analysis to tNAA, for which we found no significant differences between conditions (**Fig. 3c**). We then applied a sliding temporal window analysis to the data to test for dynamic trends in metabolite concentration. We found that in the visual stimulation condition there was an increase in Glx (max difference=1.9%, $t_{(25)}$=2.58, P=.019) and tNAA (max difference=0.1%, $t_{(25)}$=4.03, P=4.3e^{-4}), however, we found no other significant differences for GABA+, Glx, or tNAA across the three conditions (**Fig. 3d-f**). The eyes closed and eyes

open (in darkness) conditions of the K-dataset are analogous to the primary visual cortex dataset in the presented in the previous analyses, as in both there is a deprivation of visual stimulation. Thus, we may have expected to find a similar pattern of results, i.e., a decrease in GABA+ and an increase in Glx. However, the scan duration of the K-dataset was only two thirds that of ours. Indeed, in the period captured by the sliding window analysis of the K-dataset, Glx in the primary visual cortex dataset had not yet significantly risen above zero and GABA+ had only just begun to reduce significantly below zero (**Fig. 3d**, dotted lines). Further, there are fewer than half the number of participants in the K-dataset, thus less power to detect a difference. Despite these differences, the numerical pattern of results from the closed eyes and open eyes (in darkness) conditions of the K-dataset are similar to ours: the average change in concentration GABA+ and Glx is always negative and positive, respectively. By contrast, while in the visual stimulation condition the average change in concentration of Glx is always positive, GABA+ is less consistently negative than in the other two conditions.

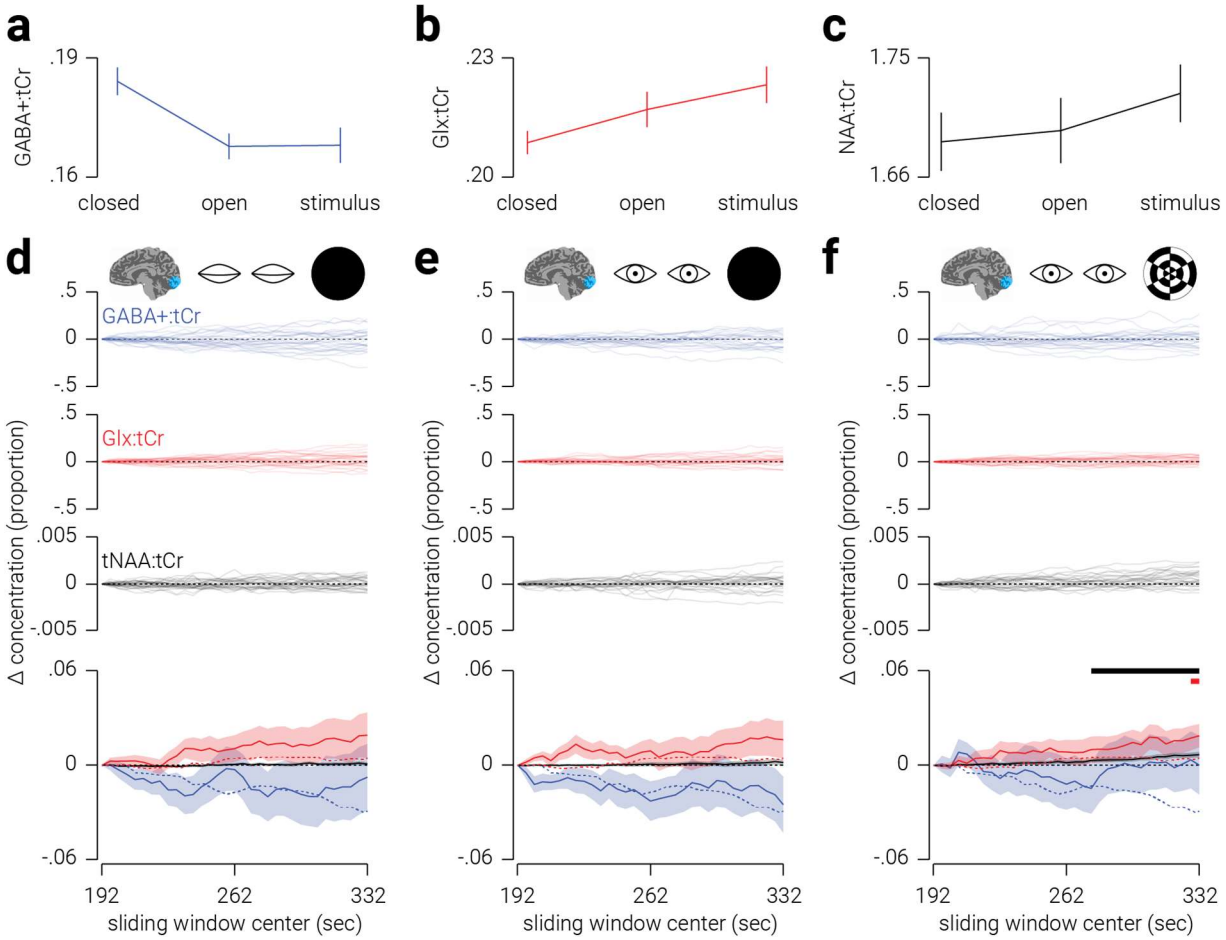

Figure 3. Low resolution temporal dynamics of metabolites in visual cortex during different viewing conditions. Static average concentration of (**a**) GABA+, (**b**) Glx, and (**c**) tNAA measured from a MRS voxel targeting the visual cortex when participants have their eyes closed, open in darkness, or open while viewing a dynamic checkerboard stimulus; data is reanalysed from (Kurcyus et al., 2018). (**d**, top) Individual traces showing change in GABA+, Glx, and tNAA in the visual cortex when participants have their eyes closed. (**d**, bottom) Same as (**d**, top), but averaged across participants. For comparison, the dotted lines show the results from the visual cortex dataset of the main analysis. (**e** & **f**) Same as (**d**), but while participants have their eyes open in (**e**) darkness or (**f**) while viewing a dynamic checkerboard stimulus. All metabolite concentrations are referenced to tCr. Error bars in (**a**-**c**) and shaded regions in (**d**-**f**) indicate s.e.m. and horizontal coloured bars at the top and bottom of (**f**) indicate (cluster corrected) periods of significant difference from zero.

High resolution temporal dynamics of GABA and Glx

In the previous analysis we used a temporal sliding window to measure change in metabolite concentrations over time. The signal-to-noise ratio of MRS measurements constrains the minimum window size that can be applied with this analysis. To overcome this limitation, we used a novel approach in which measurements are combined across subjects to achieve the maximum temporal resolution afforded by the relaxation time of the acquisition, e.g., 3 sec. In the visual cortex, we found change in GABA+, relative from the first measurement, was primarily negative, with a minimum of -20%, while change in Glx was primarily positive, with maximum of 7% (**Fig. 4a**). These results are consistent with those from the previous analysis, except the higher temporal resolution obtained with the current

approach revealed considerably larger changes in metabolite concentration than the previous estimates, which were likely obscured by smoothing measurements across the temporal window. In the posterior cingulate cortex, we found that change in both GABA+ and Glx was primarily negative, and similar in amplitude (**Fig. 4b**).

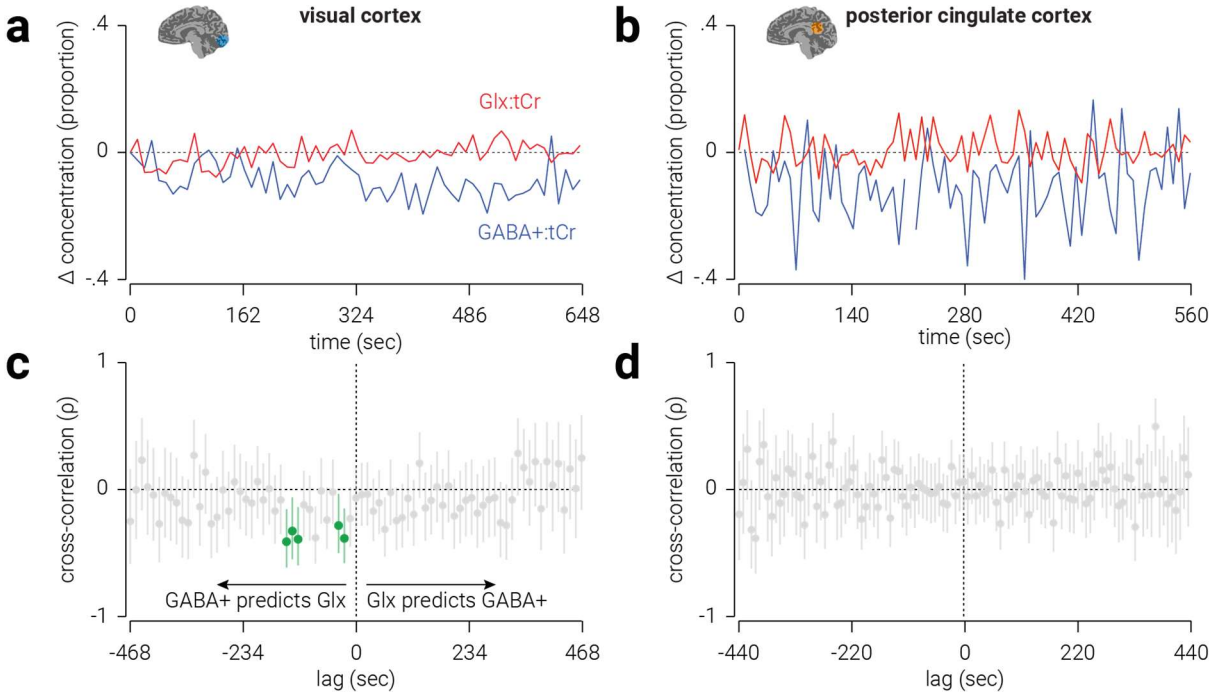

Figure 4. High resolution temporal dynamics of metabolites in visual and posterior cingulate cortex. Change in GABA+ and Glx concentration measured from voxels targeting (**a**) visual and (**b**) posterior cingulate cortices. (**c-d**) Cross-correlations between GABA+ and Glx concentration measured from voxels targeting (**c**) visual and (**d**) posterior cingulate cortices. Lag values indicate the duration between when the GABA+ measurements were acquired and the Glx measurements were acquired. Correlations at negative lags indicate GABA+ concentration predicts Glx concentration and correlations at positive lags indicate Glx predicts GABA+. Vertical lines indicate 95% confidence intervals; cluster-corrected correlations that are significantly different than zero are highlighted in green. All values are referenced to tCr.

While GABA and Glx are thought to support opposing mechanisms in the central nervous system, i.e., inhibition and excitation, it seems reasonable to expect interactions between these metabolites. For example, Gln is a primary source of GABA synthesis (Patel et al., 2001; Paulsen et al., 1988; Rae et al., 2003). Indeed, we found that the static concentration of GABA+ and Glx were positively related in the posterior cingulate cortex. However, we found no evidence for a relationship between the overall changes in these metabolites in either the visual or posterior cingulate cortex (**Table 2**). One reason for this may be that the relationship between these metabolites may only be observed at a temporally high resolution, but not averaged across a 12/13 minute period. To test this hypothesis, we used the high temporal resolution metabolite measurements to perform cross-correlation analyses on GABA+ and Glx concentration.

For the visual cortex, we found that the concentration of GABA+ predicted that of Glx during two periods of latency (**Fig. 4c**, green markers). The first period was between 24-36 sec (n(time points)=[62,61], Pearson *r*=[-.36,-.28], *P*=[.005,.029]) and the second period was between 120-144 sec (n(time points)=[54,53,52], Pearson *r*=[-.34,-.32,-.39], *P*=[.011,.019,.004]). This relationship was consistently negative, that is, a positive/negative change in GABA+ predicted a later change in Glx in the opposite direction. By contrast, we found no periods of latency in which Glx predicted the concentration of GABA+. For the posterior cingulate cortex, we found no periods of latency in which there was a significant relationship between GABA+ and Glx (**Fig. 4d**).

A possible concern is that the relationship between GABA+ and Glx was the influenced by their common reference metabolite (tCr). However, we found the same pattern of results when tNAA, rather than tCr, was used as a reference metabolite (**Fig. 5a**). Another possible concern with this new analysis is that the signal-to-noise ratio is insufficiently high to yield valid measurements, e.g., due to poor peak fitting. To assess the validity of the measurements, we attempted to reproduce the results from the low-resolution temporal analysis by applying a sliding window to the high-resolution metabolite trace. If the high-resolution measurements are valid, we should see a correspondence between the average results from the low-resolution analysis and those produced by applying a sliding temporal window to the high-resolution measurements. For the visual cortex, we found a high correlation between the measurements produced by the two analyses for both GABA+ (n=65, r=.979, P<1.0e^{-10}; **Fig. 5b**, top) and Glx (n=65, r=.993, P<1.0e^{-10}). These results support the validity of the high-resolution measurements and the results of the cross-correlation analysis.

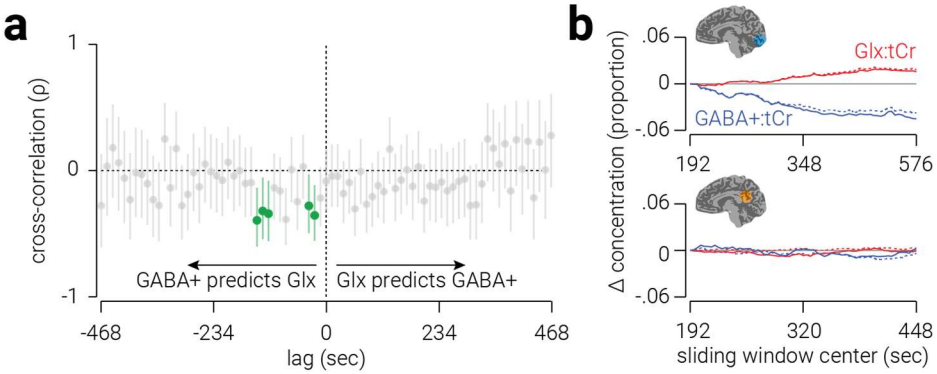

Figure 5. Controls for high resolution analyses. (**a**) Cross-correlations between GABA+ and Glx, referenced to tNAA, measured from voxels targeting visual cortex. Vertical lines indicate 95% confidence intervals; cluster-corrected correlations that are significantly different than zero are highlighted in green, correlations at negative lags indicate GABA+ predicts Glx and correlations at positive lags indicate Glx predicts GABA+. (**b**) Comparison between results from sliding window method used in the low temporal resolution analysis (dashed lines) and sliding window applied to results from high resolution analysis (solid lines) for (**b**, top) visual and (**b**, bottom) posterior cingulate cortices.

DISCUSSION

MRS can be used in vivo to quantify metabolite concentration and provide evidence for the involvement of different neurotransmitter systems, e.g., inhibitory and excitatory, in sensory and cognitive processes. In MRS studies, temporal resolution is typically sacrificed to achieve sufficient signal-to-noise ratio to produce a reliable estimate of metabolite concentration. Here we use novel analyses with large datasets to reveal the dynamics of GABA+ and Glx in visual and posterior cingulate cortices. We replicate previously established relationships between metabolites measured using the standard approach. We use a sliding window approach to show that under conditions of binocular visual deprivation, the dynamic concentrations of GABA+ and Glx in the visual cortex drifts in opposite directions, that is, GABA+ decreases while Glx increases over time. We then use a new method of combining MRS measurements across subjects, as opposed to time, to produce a high temporal resolution index of metabolite concentration. Using this approach, we find that in the visual cortex, a change in the concentration of GABA+ predicts the opposite change in Glx ~30 and ~120 sec later, e.g., an increase in GABA+ is correlated with a subsequent reduction in Glx.

Dynamic response of GABA and Glx in the visual cortex

Several studies have investigated GABA and/or Glx/Glu concentration in the visual cortex in response to different viewing conditions. Mekle et al. (2017) found a ~5% reduction in GABA concentration in response to visual stimulation. By contrast, while Kurcyus et al. (2018) reported that GABA was 16% lower when participants had their eyes open with no visual stimulation compared to when closed, they, like others (Bednařík et al., 2018, 2015; Mangia et al., 2007; Schaller et al., 2013), found no evidence for a difference in GABA in response to visual stimulation. Based on these somewhat inconsistent findings, one may infer that visual stimulation, or merely having the eyes open, leads to a reduction in the concentration of GABA in the visual cortex. Extending this rationale, one could predict that closing the eyes should produce an increase in GABA. By contrast, we found the opposite result: during a 13 min period of resting in which participants' eyes were closed, the concentration of GABA+ in the visual cortex reduced on average by 4.5%.

Our reanalysis of data comparing metabolite concentration in the visual cortex under different viewing conditions suggests that these results may not be mutually exclusive. Consistent with the original study (Kurcyus et al., 2018), we found that static measurements of GABA+ indicated concentrations were higher when participants had their eyes closed. Despite this, dynamic analysis of the data indicated a trend towards reduction in concentration over time. This pattern of results was more consistent when participants had their eyes closed than during visual stimulation. Indeed, our results are consistent with previous work showing

that monocular deprivation leads to reduced GABA concentration (~8%) in the visual cortex, but not the posterior cingulate cortex, relative a pre-deprivation baseline measurement (Lunghi et al., 2015b). Thus, our finding that GABA is reduced when both eyes are closed may indicate that visual deprivation, either monocular or binocular, evokes a reduction in the concentration of GABA in the visual cortex.

Previous observations of Glx concentration in the visual cortex have been more consistent; several studies have shown Glx/Glu concentration increases (2-4%) in response to visual stimulation (Bednařík et al., 2018, 2015; Ip et al., 2017; Kurcyus et al., 2018; Lin et al., 2012; Mangia et al., 2007; Schaller et al., 2013). Increased Glu in the visual cortex, evoked by visual stimulation, has been linked to increased blood-oxygenation level dependent responses (Ip et al., 2017). Further, here we measured Glx, a complex comprising Glu and Gln, and previous 7T MRS work suggests that visual stimulation evoked changes in Glu, but not Gln, in the visual cortex (Bednařík et al., 2018, 2015; Schaller et al., 2013). It is possible that the increase in Glx we found here, which occurred in the absence of visual stimulation, was driven by an alternative mechanism, one that is unrelated to BOLD activity and/or reflects changes in Gln rather than Glu. More work is needed it disambiguate changes in metabolite concentration that occur in the visual cortex at different time scales and under different viewing conditions. For instance, future work could combine fMRI and MRS measurements to test whether the phenomenon observed here is related to BOLD activity (Ip et al., 2017).

To produce a high temporal resolution measure of metabolite concentrations, we applied a novel approach in which we combined MRS transients across subjects, rather than time. This approach yields a single measurement of metabolite concentration as a function of time; thus, we cannot test the statistical significance of the changes observed over time. However, it is reasonable to assume that the changes observed using the sliding temporal window or static approaches underestimate the true magnitude of change, due to averaging. Measurements produced by combining transients across subjects provide an indication of the true magnitude of change in GABA+ and Glx during the scan: up to 20% for GABA+ and 7% for Glx.

Dynamic relationship between GABA and Glx

A common factor of studies of GABA and Glx/Glu in the visual cortex is that these metabolites consistently change in opposite directions, and not in the same direction (Kurcyus et al., 2018; Mekle et al., 2017; Rideaux et al., 2019). This pattern would suggest an interdependency between the two metabolites. Given that Gln is a primary source of GABA synthesis (Patel et al., 2001; Paulsen et al., 1988; Rae et al., 2003), one may expect that a change in the concentration of GABA may result in a corresponding change in Glx (Gln and Glu), or vice versa. In line with this, our high temporal resolution analysis of the data revealed

a striking cross-correlation between these metabolites in the visual cortex. Specifically, we found that the concentration of GABA+ predicts the concentration of Glx ~30 and ~120 sec later. This relationship, which accounts for up to ~20% of the variance of Glx, is obscured by conventional approaches of MRS analysis; indeed, we found no evidence for a relationship between the overall change in GABA+ and Glx.

A limitation of MRS is that it measures the total concentration of neurochemicals within a localized region and cannot distinguish between intracellular and extracellular pools of GABA. It is generally thought that intracellular vesicular GABA drives neurotransmission (Belelli et al., 2009), whereas extracellular GABA maintains tonic cortical inhibition (Martin and Rimvall, 1993). Synthesis of intracellular GABA from Gln via the GABA-Gln cycle occurs on the scale of milliseconds, so it seems unlikely that this metabolic association could explain the predictive relationship between GABA and Glx concentration ~30 and ~120 sec later. Instead, this relationship may reflect changes in the level of extracellular GABA, followed by relatively sluggish changes in the concentration of Glu to maintain the balance of inhibition and excitation.

Conclusion

The relatively low signal-to-noise of MRS measurements has shaped the types of questions that the technique has been used to address. Here we overcome this limitation by combining data from large cohorts to examine the dynamics of GABA and Glx concentration in the visual cortex. Through use of existing and novel analyses, we reveal opposing dynamic shifts in GABA and Glx in the visual cortex while participants are at rest. Further, we demonstrate a predictive relationship between GABA and Glx that is present in both visual and posterior cingulate cortices. This study exposes temporal trends of primary neurotransmitters in the visual cortex, and more generally, these findings demonstrate the feasibility of using MRS to investigate in vivo dynamic changes of metabolites.

Acknowledgements

The work was supported by the Leverhulme Trust (ECF-2017-573), the Issac Newton Trust (17.08(o)), and the Wellcome Trust (095183/Z/10/Z). I acknowledge the assistance of Katarzyna Kurcyus, Valentin Riedl, Mark Mikkelsen, and Richard Edden in supplying their data for reanalysis.

REFERENCES

Bednařík P, Tkáč I, Giove F, Dinuzzo M, Deelchand DK, Emir UE, Eberly LE, Mangia S. 2015. Neurochemical and BOLD responses during neuronal activation measured in the human visual cortex at 7 Tesla. *J Cereb Blood Flow Metab* **35**:601–610. doi:10.1038/jcbfm.2014.233

Bednařík P, Tkáč I, Giove F, Eberly LE, Deelchand DK, Barreto FR, Mangia S. 2018. Neurochemical responses to chromatic and achromatic stimuli in the human visual cortex. *J Cereb Blood Flow Metab* **38**:347–359. doi:10.1177/0271678X17695291

Belelli D, Harrison NL, Maguire J, Macdonald RL, Walker MC, Cope DW. 2009. Extrasynaptic GABAA Receptors: Form, Pharmacology, and Function. *J Neurosci* **29**:12757–12763. doi:10.1523/JNEUROSCI.3340-09.2009

Bhattacharyya PK, Lowe MJ, Phillips MD. 2007. Spectral quality control in motion-corrupted single-voxel J-difference editing scans: An interleaved navigator approach. *Magn Reson Med* **58**:808–812. doi:10.1002/mrm.21337

Bonett DG, Wright TA. 2000. Sample size requirements for estimating Pearson, Kendall and Spearman correlations. *Psychometrika* **65**:23–28. doi:10.1007/BF02294183

Boroojerdi B, Battaglia F, Muellbacher W, Cohen LG. 2001. Mechanisms underlying rapid experience-dependent plasticity in the human visual cortex. *Proc Natl Acad Sci U S A* **98**:14698–14701. doi:10.1073/pnas.251357198

Boroojerdi B, Bushara KO, Corwell B, Immisch I, Battaglia F, Muellbacher W, Cohen LG. 2000. Enhanced Excitability of the Human Visual Cortex Induced by Short-term Light Deprivation. *Cereb Cortex* **10**:529–534. doi:10.1093/cercor/10.5.529

Edden RAE, Muthukumaraswamy SD, Freeman TCA, Singh KD. 2009. Orientation Discrimination Performance Is Predicted by GABA Concentration and Gamma Oscillation Frequency in Human Primary Visual Cortex. *J Neurosci* **29**:15721–15726. doi:10.1523/JNEUROSCI.4426-09.2009

Edden RAE, Puts NAJ, Harris AD, Barker PB, Evans CJ. 2014. Gannet: A batch-processing tool for the quantitative analysis of gamma-aminobutyric acid-edited MR spectroscopy spectra. *J Magn Reson Imaging* **40**:1445–1452. doi:10.1002/jmri.24478

Harris AD, Puts NAJ, Edden RAE. 2015. Tissue correction for GABA-edited MRS: Considerations of voxel composition, tissue segmentation, and tissue relaxations. *J Magn Reson Imaging* **42**:1431–1440. doi:10.1002/jmri.24903

He HY, Hodos W, Quinlan EM. 2006. Visual deprivation reactivates rapid ocular dominance plasticity in adult visual cortex. *J Neurosci* **26**:2951–2955. doi:10.1523/JNEUROSCI.5554-05.2006

Huang S, Gu Y, Quinlan EM, Kirkwood A. 2010. A refractory period for rejuvenating GABAergic synaptic transmission and ocular dominance plasticity with dark exposure. *J Neurosci* **30**:16636–16642. doi:10.1523/JNEUROSCI.4384-10.2010

Ip IB, Berrington A, Hess AT, Parker AJ, Emir UE, Bridge H. 2017. Combined fMRI-MRS acquires

549 simultaneous glutamate and BOLD-fMRI signals in the human brain. *Neuroimage* **155**:113–119.
550 doi:10.1016/J.NEUROIMAGE.2017.04.030

551 Jansen JFA, Backes WH, Nicolay K, Kooi ME. 2006. ^{1}H MR Spectroscopy of the Brain: Absolute
552 Quantification of Metabolites. *Radiology* **240**:318–332. doi:10.1148/radiol.2402050314

553 Kurcyus K, Annac E, Hanning NM, Harris AD, Oeltzschner G, Edden RAE, Riedl V. 2018. Opposite
554 Dynamics of GABA and Glutamate Levels in the Occipital Cortex during Visual Processing. *J*
555 *Neurosci* **38**:9967–9976. doi:10.1523/JNEUROSCI.1214-18.2018

556 Lange T, Zaitsev M, Buechert M. 2011. Correction of frequency drifts induced by gradient heating in
557 1H spectra using interleaved reference spectroscopy. *J Magn Reson Imaging* **33**:748–754.
558 doi:10.1002/jmri.22471

559 Lin Y, Stephenson MC, Xin L, Napolitano A, Morris PG. 2012. Investigating the metabolic changes
560 due to visual stimulation using functional proton magnetic resonance spectroscopy at 7 T. *J*
561 *Cereb Blood Flow Metab* **32**:1484–1495. doi:10.1038/jcbfm.2012.33

562 Lunghi C, Berchicci M, Morrone MC, Di Russo F. 2015a. Short-term monocular deprivation alters
563 early components of visual evoked potentials. *J Physiol* **593**:4361–4372. doi:10.1113/JP270950

564 Lunghi C, Emir UE, Morrone MC, Bridge H. 2015b. Short-Term monocular deprivation alters GABA in
565 the adult human visual cortex. *Curr Biol*. doi:10.1016/j.cub.2015.04.021

566 Mangia S, Tkáč I, Gruetter R, Van de Moortele P-F, Maraviglia B, Uğurbil K. 2007. Sustained
567 Neuronal Activation Raises Oxidative Metabolism to a New Steady-State Level: Evidence from ^{1}
568 H NMR Spectroscopy in the Human Visual Cortex. *J Cereb Blood Flow Metab* **27**:1055–1063.
569 doi:10.1038/sj.jcbfm.9600401

570 Martin DL, Rimvall K. 1993. Regulation of γ-Aminobutyric Acid Synthesis in the Brain. *J Neurochem*.
571 doi:10.1111/j.1471-4159.1993.tb03165.x

572 Mekle R, Kühn S, Pfeiffer H, Aydin S, Schubert F, Ittermann B. 2017. Detection of metabolite changes
573 in response to a varying visual stimulation paradigm using short-TE 1H MRS at 7 T. *NMR*
574 *Biomed* **30**:e3672. doi:10.1002/nbm.3672

575 Mescher M, Merkle H, Kirsch J, Garwood M, Gruetter R. 1998. Simultaneous in vivo spectral editing
576 and water suppression. *NMR Biomed* **11**:266–272. doi:10.1002/(SICI)1099-
577 1492(199810)11:6<266::AID-NBM530>3.0.CO;2-J

578 Mescher M, Tannus A, O'Neil Johnson M, Garwood M. 1996. Solvent suppression using selective
579 echo dephasing. *J Magn Reson - Ser A* **123**:226–229. doi:10.1006/jmra.1996.0242

580 Mikkelsen M, Barker PB, Bhattacharyya PK, Brix MK, Buur PF, Cecil KM, Chan KL, Chen DYT,
581 Craven AR, Cuypers K, Dacko M, Duncan NW, Dydak U, Edmondson DA, Ende G, Ersland L,
582 Gao F, Greenhouse I, Harris AD, He N, Heba S, Hoggard N, Hsu T-W, Jansen JFA, Kangarlu A,
583 Lange T, Lebel RM, Li Y, Lin C-YE, Liou J-K, Lirng J-F, Liu F, Ma R, Maes C, Moreno-Ortega M,
584 Murray SO, Noah S, Noeske R, Noseworthy MD, Oeltzschner G, Prisciandaro JJ, Puts NAJ,
585 Roberts TPL, Sack M, Sailasuta N, Saleh MG, Schallmo M-P, Simard N, Swinnen SP,

586 Tegenthoff M, Truong P, Wang G, Wilkinson ID, Wittsack H-J, Xu H, Yan F, Zhang C,
587 Zipunnikov V, Zöllner HJ, Edden RAE. 2017. Big GABA: Edited MR spectroscopy at 24 research
588 sites. *Neuroimage* **159**:32–45. doi:10.1016/j.neuroimage.2017.07.021

589 Mikkelsen M, Harris AD, Edden RAE, Puts NAJ. 2018a. Macromolecule-suppressed GABA
590 measurements correlate more strongly with behavior than macromolecule-contaminated
591 GABA+ measurements. *Brain Res* **1701**:204–211. doi:10.1016/J.BRAINRES.2018.09.021

592 Mikkelsen M, Loo RS, Puts NAJ, Edden RAE, Harris AD. 2018b. Designing GABA-edited magnetic
593 resonance spectroscopy studies: Considerations of scan duration, signal-to-noise ratio and
594 sample size. *J Neurosci Methods*. doi:10.1016/j.jneumeth.2018.02.012

595 Mikkelsen M, Rimbault DL, Barker PB, Bhattacharyya PK, Brix MK, Buur PF, Cecil KM, Chan KL,
596 Chen DYT, Craven AR, Cuypers K, Dacko M, Duncan NW, Dydak U, Edmondson DA, Ende G,
597 Ersland L, Forbes MA, Gao F, Greenhouse I, Harris AD, He N, Heba S, Hoggard N, Hsu T-W,
598 Jansen JFA, Kangarlu A, Lange T, Lebel RM, Li Y, Lin C-YE, Liou J-K, Lirng J-F, Liu F, Long
599 JR, Ma R, Maes C, Moreno-Ortega M, Murray SO, Noah S, Noeske R, Noseworthy MD,
600 Oeltzschner G, Porges EC, Prisciandaro JJ, Puts NAJ, Roberts TPL, Sack M, Sailasuta N,
601 Saleh MG, Schallmo M-P, Simard N, Stoffers D, Swinnen SP, Tegenthoff M, Truong P, Wang G,
602 Wilkinson ID, Wittsack H-J, Woods AJ, Xu H, Yan F, Zhang C, Zipunnikov V, Zöllner HJ, Edden
603 RAE. 2019. Big GABA II: Water-referenced edited MR spectroscopy at 25 research sites.
604 *Neuroimage* **191**:537–548. doi:10.1016/J.NEUROIMAGE.2019.02.059

605 Mullins PG, McGonigle DJ, O'Gorman RL, Puts NAJ, Vidyasagar R, Evans CJ, Edden RAE, Brookes
606 MJ, Garcia A, Foerster BR, Petrou M, Price D, Solanky BS, Violante IR, Williams S, Wilson M.
607 2014. Current practice in the use of MEGA-PRESS spectroscopy for the detection of GABA.
608 *Neuroimage* **86**:43–52. doi:10.1016/j.neuroimage.2012.12.004

609 Patel AB, Rothman DL, Cline GW, Behar KL. 2001. Glutamine is the major precursor for GABA
610 synthesis in rat neocortex in vivo following acute GABA-transaminase inhibition. *Brain Res*
611 **919**:207–220. doi:10.1016/S0006-8993(01)03015-3

612 Paulsen RE, Odden E, Fonnum F. 1988. Importance of glutamine for gamma-aminobutyric acid
613 synthesis in rat neostriatum in vivo. *J Neurochem* **51**:1294–9. doi:10.1111/j.1471-
614 4159.1988.tb03099.x

615 Puts NAJ, Edden RAE. 2012. In vivo magnetic resonance spectroscopy of GABA: A methodological
616 review. *Prog Nucl Magn Reson Spectrosc* **60**:29–41. doi:10.1016/j.pnmrs.2011.06.001

617 Rae C, Hare N, Bubb WA, McEwan SR, Bröer A, McQuillan JA, Balcar VJ, Conigrave AD, Bröer S.
618 2003. Inhibition of glutamine transport depletes glutamate and GABA neurotransmitter pools:
619 Further evidence for metabolic compartmentation. *J Neurochem* **85**:503–514.
620 doi:10.1046/j.1471-4159.2003.01713.x

621 Rideaux R, Goncalves NR, Welchman AE. 2019. Mixed-polarity random-dot stereograms alter GABA
622 and Glx concentration in the early visual cortex. *J Neurophysiol* **122**:888–896.
623 doi:10.1152/jn.00208.2019

624 Schaller B, Mekle R, Xin L, Kunz N, Gruetter R. 2013. Net increase of lactate and glutamate
625 concentration in activated human visual cortex detected with magnetic resonance spectroscopy
626 at 7 tesla. *J Neurosci Res* **91**:1076–1083. doi:10.1002/jnr.23194

627 Tkáč I, Gruetter R. 2005. Methodology of 1H NMR spectroscopy of the human brain at very high
628 magnetic fields. *Appl Magn Reson* **29**:139–157. doi:10.1007/BF03166960